Supporting Information for "Endocytosis efficiency and targeting ability by cooperation of nanoparticles"

Teng Ma
Qingdao Innovation and Development Base, Harbin Engineering University
1777 Sansha Road, West Coast New Area, Qingdao 266000, China
College of Materials Science and Chemical Engineering, Harbin Engineering University
145 Nantong Street, Nangang District, Harbin 150001, China
mateng_hrbeu@hrbeu.edu.cn

Tianjiao Chen
Qingdao Innovation and Development Base, Harbin Engineering University
1777 Sansha Road, West Coast New Area, Qingdao 266000, China
18974690106@163.com

Huifeng Tan
Center for Composite Materials, Harbin Institute of Technology
National Key Laboratory of Science and Technology on Advanced Composites in Special Environments, Harbin Institute of Technology
92 Xidazhi Street, Nangang District, Harbin 150001, China
tanhf@hit.edu.cn

Songsong Zhang [1]
Qingdao Innovation and Development Base, Harbin Engineering University
1777 Sansha Road, West Coast New Area, Qingdao 266000, China
zhangss55555@163.com

Hao Wei [2]
Qingdao Innovation and Development Base, Harbin Engineering University
1777 Sansha Road, West Coast New Area, Qingdao 266000, China
weihao@hrbeu.edu.cn

Qiang Wang
Qingdao Innovation and Development Base, Harbin Engineering University
1777 Sansha Road, West Coast New Area, Qingdao 266000, China
13864285521@126.com

Zhijia Zhang
Qingdao Innovation and Development Base, Harbin Engineering University
1777 Sansha Road, West Coast New Area, Qingdao 266000, China

[1] Corresponding author.
[2] Corresponding author.

zhijia.zhang@hrbeu.edu.cn

Wenjun Zhou
Qingdao Innovation and Development Base, Harbin Engineering University
1777 Sansha Road, West Coast New Area, Qingdao 266000, China
College of Materials Science and Chemical Engineering, Harbin Engineering University
145 Nantong Street, Nangang District, Harbin 150001, China
wjzhou2012@163.com

Lin Wang
Qingdao Innovation and Development Base, Harbin Engineering University
1777 Sansha Road, West Coast New Area, Qingdao 266000, China
linwang@hrbeu.edu.cn

Guojun Wang
Qingdao Innovation and Development Base, Harbin Engineering University
1777 Sansha Road, West Coast New Area, Qingdao 266000, China
wang5347@hrbeu.edu.cn

1. One-bead coarse-grained lipid model

We adopt the one-bead coarse-grained lipid model developed by Yuan et al.[1, 2], which can describe the dynamics without losing physical properties of lipid bilayer membrane but reduce the computational cost greatly. The model has been used to capture the gel-fluid-gas phase transitions of lipids, diffusion, bending rigidity and other mechanical properties of a lipid bilayer membrane successfully [1]. The interaction potential between coarse-grained lipid particles depends on their relative distance and orientation and can be expressed as:

$$U(r_{ij},n_i,n_j)=\begin{cases}u_R(r)+\left[1-\phi(\hat{r}_{ij},n_i,n_j)\right], & r<r_{min},\\ u_A(r)\phi(\hat{r}_{ij},n_i,n_j), & r_{min}<r<r_c,\end{cases} \tag{1}$$

where r_{ij} is the relative distance vector between two beads r_i and r_j, n_i and n_j represent the corresponding normal vectors and $\hat{r}_{ij}=\frac{r_{ij}}{r}$. r_c is the cutoff distance and r_{min} is the distance which minimizes the potential energy $u_A(r)$. $u_R(r)$ and $u_A(r)$ are the repulsive potential and attractive potential given by the following formula,

$$u_R(r)=\epsilon\left[\left(\frac{r_{min}}{r}\right)^4-2\left(\frac{r_{min}}{r}\right)^2\right], \tag{2}$$

$$u_A(r)=-\epsilon\cos^{2\eta}\left(\frac{\pi\left(r-r_{min}\right)}{2\left(r_c-r_{min}\right)}\right) \tag{3}$$

where ϵ is the energy unit and $r_{min}=2^{1/6}\sigma$ with σ being the length unit. The exponent η controls the slope of the attractive potential.

The angular function ϕ is

$$\phi(\hat{r}_{ij},n_i,n_j)=1+\mu\left(a(\hat{r}_{ij},n_i,n_j)-1\right) \tag{4}$$

$$a(\hat{r}_{ij},n_i,n_j)=\left(n_i\times\hat{r}_{ij}\right)\cdot\left(n_j\times\hat{r}_{ij}\right)+sin\theta_0(n_i-n_j)\cdot\hat{r}_{ij}-sin^2\theta_0 \tag{5}$$

where $a(\hat{r}_{ij},n_i,n_j)$ is a weight function to tune the lipid interaction force by the two beads' orientation. μ controls the bending rigidity and θ_0 represents the spontaneous angle between two lipids.

2. The sphere NP model

The sphere NP is represented by a spherical shell mesh, which contains evenly distributed vertices points, edges connecting the vertex points and triangles formed by the edges[3, 4]. The total potential of the elastic NP is expressed using the in-plane energy $V_{in-plane}$, the bending energy $V_{bending}$, the area energy V_{area} and the volume energy V_{volume} as follow[5]:

$$V(x_i) = V_{in\text{-}plane} + V_{bending} + V_{area} + V_{volume} \tag{6}$$

The in-plane potential $V_{in-plane}$ describes the stretch energy of the networks using harmonic springs,

$$V_{in\text{-}plane} = \sum_{j=1}^{N_s} \left[k_s (l_j - l_{j0})^2\right] \tag{7}$$

where l_i and l_0 are the instantaneous and equilibrium length of the *i*-th spring and k_s is the spring constant. The bending energy $V_{bending}$ is written as:

$$V_{bending} = \sum_{j=1}^{N_s} k_{bend}\left[1 - \cos\left(\theta_j - \theta_{j0}\right)\right] \tag{8}$$

where k_{bend} is the bending constant, θ_j and θ_{j0} are the instantaneous and equilibrium dihedral angle between two adjacent triangles sharing a common edge. In our simulations, we tune the k_{bend} to change the rigidity of NPs.

The area potential V_{area} constraints the total area and the local area of each triangles to enforce the incompressibility of NP and is expressed as:

$$V_{area} = \frac{k_a}{2A_0^{tot}}\left(A - A_0^{tot}\right)^2 + \frac{k_d}{2A_0}\sum_{j=1}^{N_t}\left(A_j - A_0\right)^2 \tag{9}$$

and the volume constraints V_{volume} is given by

$$V_{volume} = \frac{k_v^2}{2V_0^{tot}}\left(V - V_0^{tot}\right)^2 \tag{10}$$

where k_a, k_d and k_v are constraints constants for global area, local area and global volume, A, A_j, V are the instantaneous global area, local area and global volume, A_0^{tot}, A_0, V_0^{tot} are their respective equilibrium values.

3. The ligand-receptor interaction

10% beads of the NP are evenly selected as the ligands. The ligand-receptor interaction is modeled by a bond interaction, i.e., one ligand can only bind with one receptor. One ligand-receptor bond will be created when the distance between them is less than 3.5σ. If their distance is larger than 4σ, the ligand-receptor bond will break. The potential between ligands and receptor bonds is descibed using the Morse potential[6]:

$$V_{\text{Morse}}(r) = D_0\left[1 - exp\left(-\alpha(r - r_0)\right)\right]^2 - D_0 \tag{11}$$

where r_0 is the equilibrium bond distance, α is the stiffness parameter and determines the width of the potential. D_0 is the potential well depth.

4. The force distribution of the beads on the contact edge of the phospholipid membrane and the nanoparticle

The radial and vertical force distribution of the lipid beads on the contact edges between the membrane and the NPs are shown in Fig. S 1 and Fig. S 2. We found that the smaller the curvature, i.e. the longer the contact edge length, the bigger $\overline{f}_{centripetal}$. $\overline{f}_{centripetal}$ plays an important role in pushing the lipid molecules towards the NPs. Under the push of $\overline{f}_{centripetal}$, the distance between the lipid molecules and the NPs decreases, and the interaction forces increases. For the vertical wrapping force, the more beads on the NPs located below the lipid membrane plane, the greater $\overline{f}_z$ in the downward direction. $\overline{f}_z$ accelerate the wrapping.

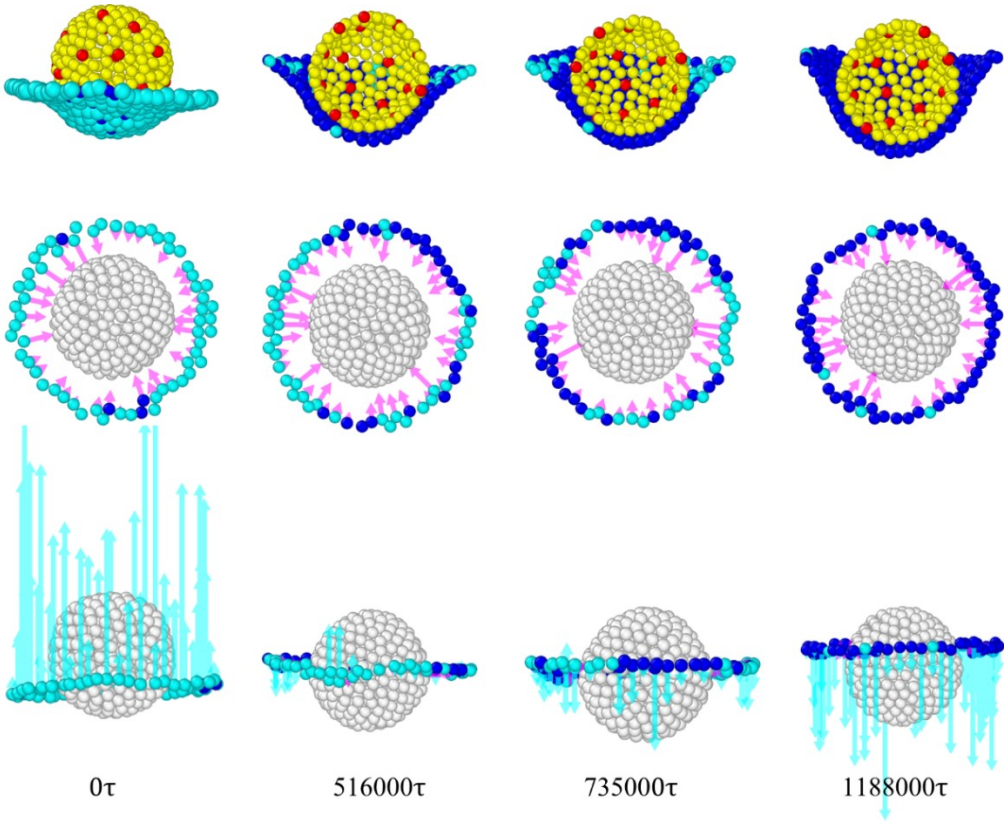

Fig. S 1 The force distribution of the beads on the contact edge of the membrane and the single NP during the wrapping.

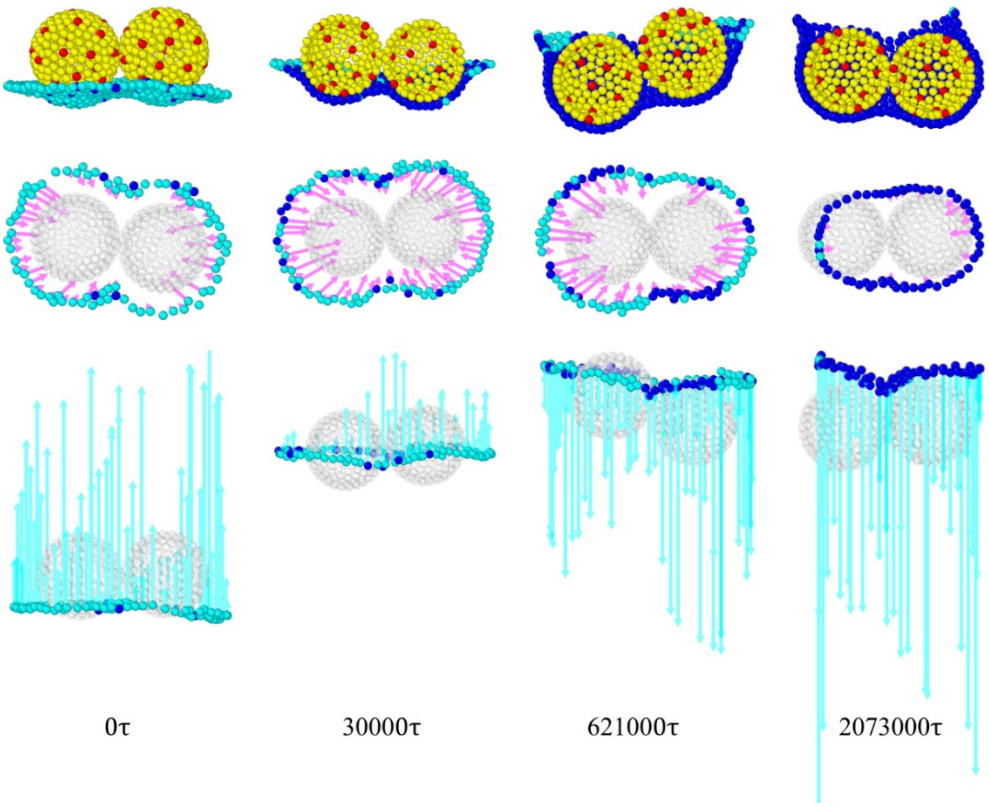

Fig. S 2 The force distribution of the beads on the contact edge of the membrane and the two NPs during the wrapping.

5. The wrapping of nanoparticles with different sizes.

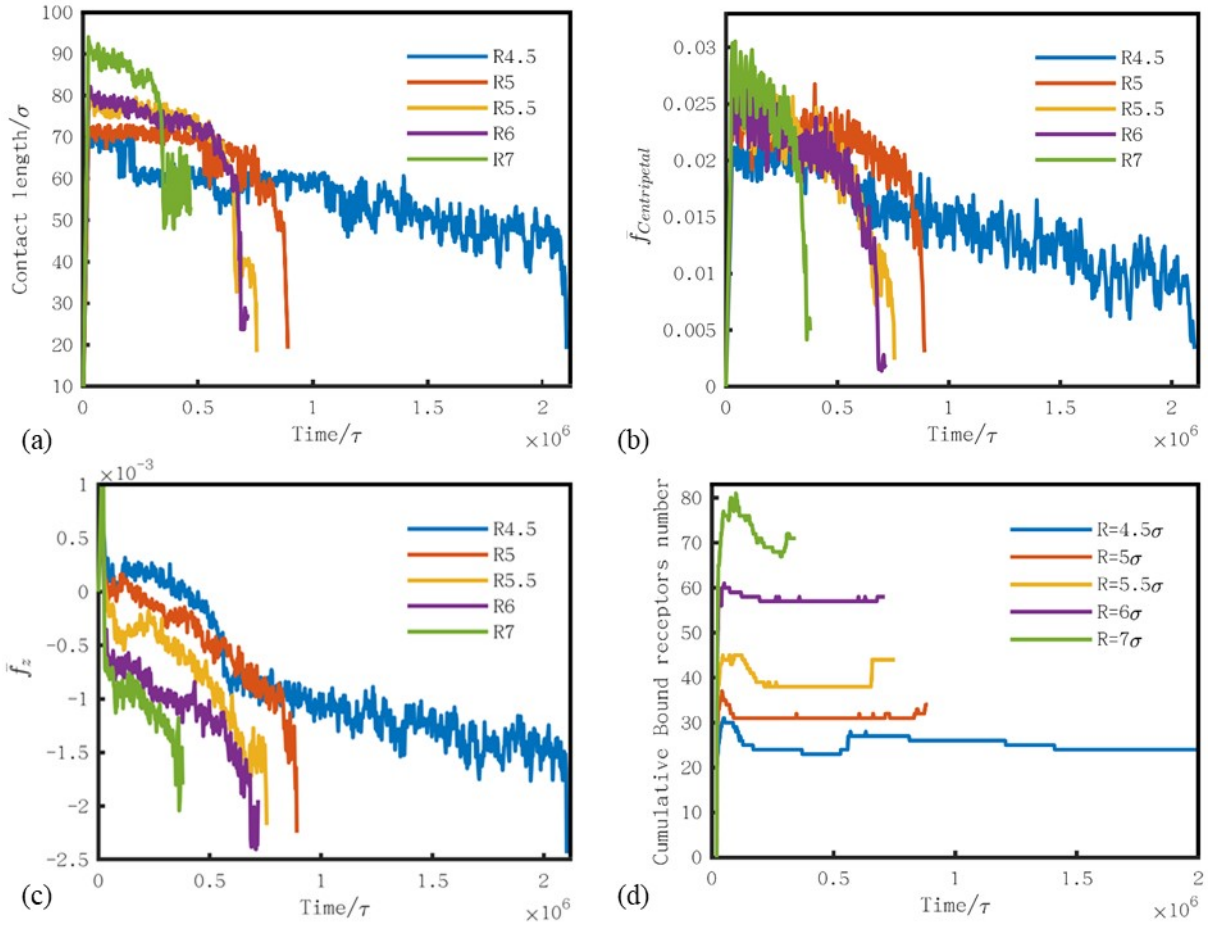

Fig. S 3 The interaction between two identical rigid nanoparticles with different radii and the phospholipid membrane. (a) Lengths of nanoparticles and membrane contact edges. (b) $\overline{f}_{centripetal}$ on the beads on the contact edges. (c) $\overline{f}_z$ on the beads on the contact edges. (d) Cumulative number of receptor-ligand bonds.

6. Phase diagram of the endocytosis state regarding single NPs' size, receptor-ligand interaction strength.

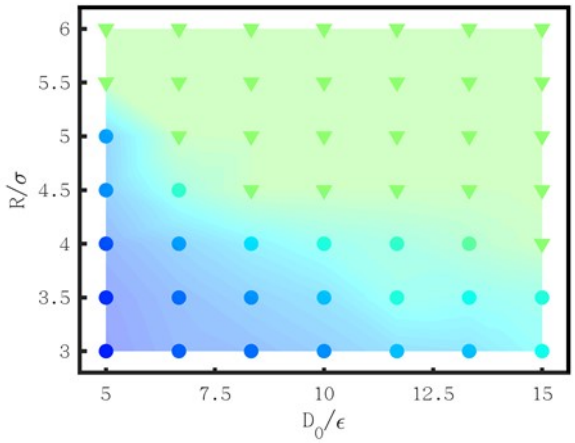

Fig. S 4 The phase diagram of endocytosis states of single nanoparticle with respect to radius and interaction strength: ● means adhesion, ▼ means endocytosis.

7. Wrapping of multiple NPs.

The snapshot of wrapping of multiple NPs with $R = 5\sigma$ are shown in Fig. S 5. For cases where NPs are arranged in a row, they will be gradually swallowed up one after another. For cases where NPs are arranged in a square packing, they will first gradually change into a hexagonal close packing form through positional changes, and further be internalized simultaneously.

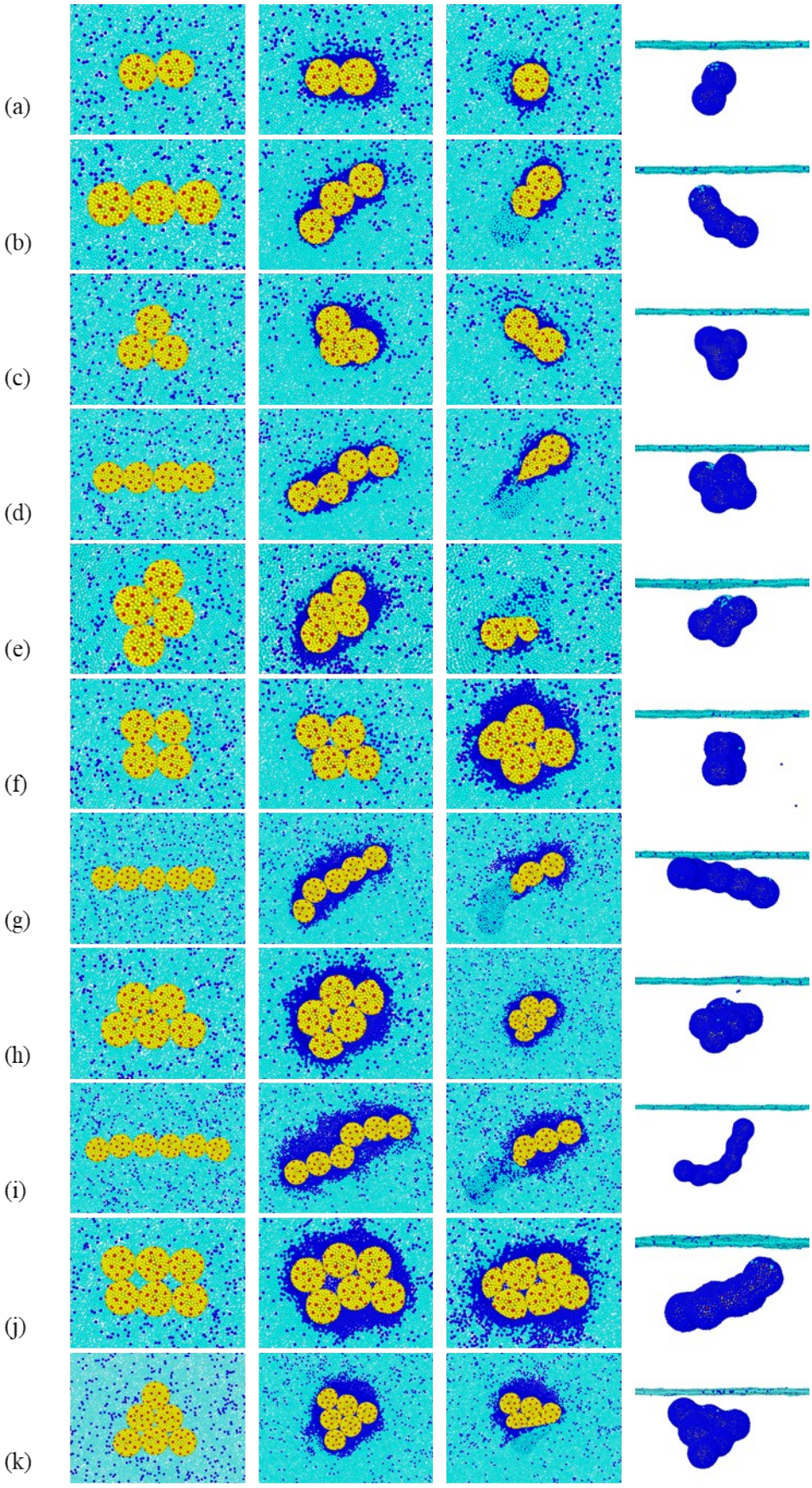

Fig. S 5 Snapshots of membrane wrapping of different numbers of spherical nanoparticles with

different arrangement. (a) $N_{NP} = 2$, arranged in a row; (b) $N_{NP} = 3$, arranged in a row; (c) $N_{NP} = 3$, hexagonal close packing; (d) $N_{NP} = 4$, arranged in a row; (e) $N_{NP} = 4$, hexagonal close packing; (f) $N_{NP} = 4$, square packing; (g) $N_{NP} = 5$, arranged in a row; (h) $N_{NP} = 5$, hexagonal close packing; (i) $N_{NP} = 6$, arranged in a row; (j) $N_{NP} = 6$, square packing; (k) $N_{NP} = 6$, hexagonal close packing.

For the endocytosis of multiple NPs, the contact length, $\overline{f}_{centripetal}$, $\overline{f}_z$, as well as the cumulative bound receptor numbers, are shown in Fig. S 6. At the beginning of contact, the nanoparticles arranged in a row have the longest contact edge length. The length of the contact boundary is similar in hexagonal and square packing arrangements. Due to the relative configurations between NPs and lipid membranes, hexagonal close packed and square packed NPs generate greater $\overline{f}_{centripetal}$ and $\overline{f}_z$ at the contact edges, resulting in faster internalization of NPs under these two arrangements.

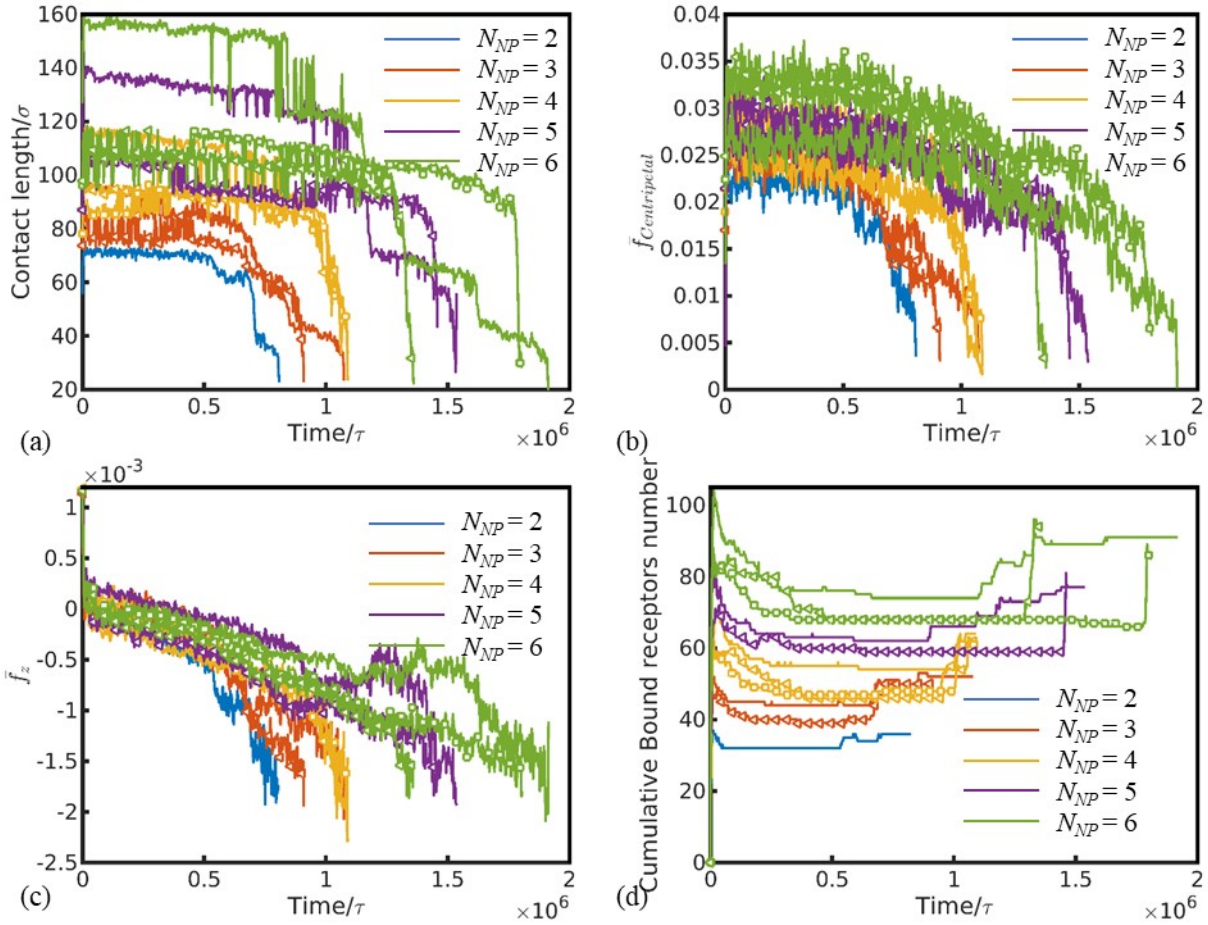

Fig. S 6 The interaction between nanoparticles and the phospholipid membrane. (a) Lengths of

nanoparticles and membrane contact edges. (b) $\overline{f}_{centripetal}$ on the beads on the contact edges. (c) $\overline{f}_{z}$ on the beads on the contact edges. (d) Cumulative number of receptor-ligand bonds. — means NPs arranged in a row, △ means NPs arranged in hexagonal close packing, □ means NPs arranged in square packing.

8. Wrapping of single elastic NP.

Fig. S 7 gives the typical wrapping ratio evolution of single elastic NP with $k_{bend} = 0.001\epsilon$ for $R = 5\sigma$ and $R = 6\sigma$. The results of rigid NPs with $k_{bend} = inf$ are also shown for comparison. For $R = 5\sigma$, though the rigid NP can be fully engulfed, the soft NP can't be wrapped totally and adheres to the membrane eventually. For $R = 6\sigma$, the soft NP need more time to be finally engulfed. The minimum size of elastic NPs that can be fully engulfed by the cell membrane is increased and the single elastic NP results in inefficient cellular uptake. These results all agree with the conclusions of Shen et al[5]. Though the sizes of NPs used in their simulations are bigger than the optimal NP size for endocytosis. The snapshot of wrapping of single NP with $R = 6\sigma$ with $k_{bend} = inf$ and $k_{bend} = 0.001\epsilon$ are shown in Fig. S 8, the NP with $k_{bend} = 0.001\epsilon$ shows significant deformation during the process compared to its rigid counterpart. The soft NP transitions from a flat shape at the bottom to a gyroscopic shape, and finally returns to a spherical shape when it is completely wrapped. Ref. [7] points out that soft NPs are deformed under the action of receptor-ligand interaction forces, resulting in lower endocytosis efficiency. The results in this paper is consistent with this conclusion. The deformation of the elastic NPs will lead to the change of the local force of the phospholipid membrane and the change of the energy barrier, which will be quantitatively expressed below.

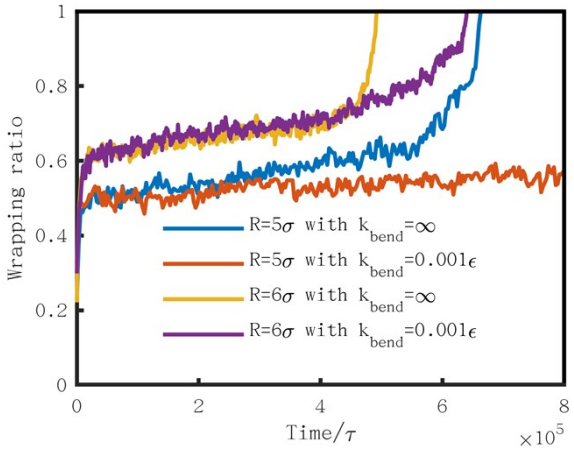

Fig. S 7 Effects of elasticity on wrapping function as time.

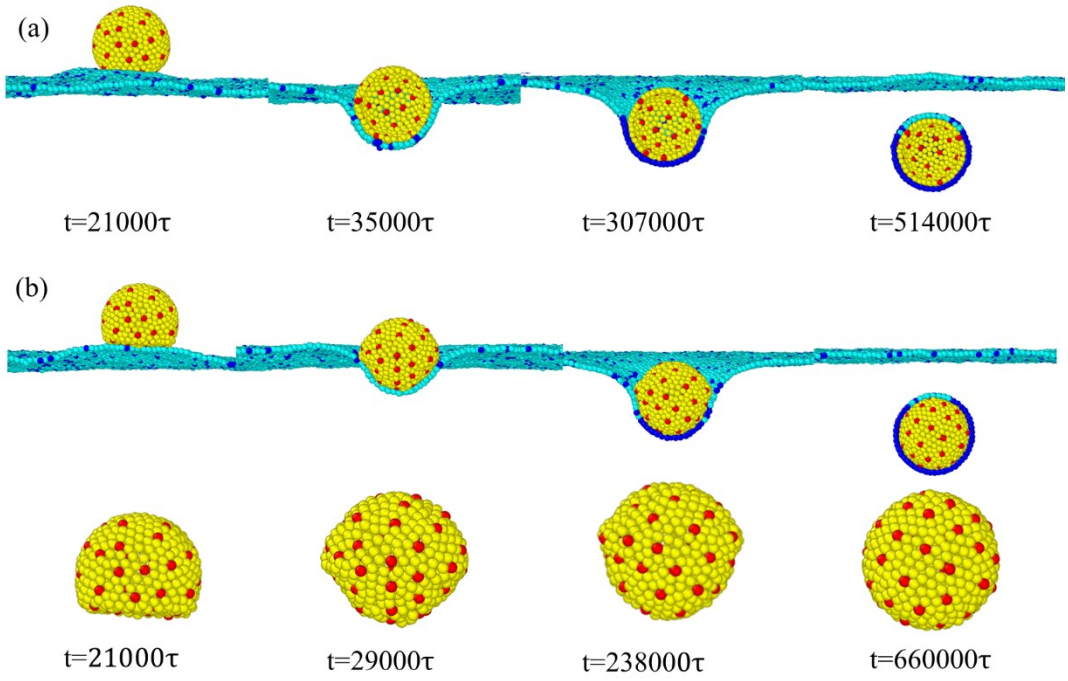

Fig. S 8 Snapshots of the membrane wrapping of single NPs. (a) one rigid NP of radius $R = 6\sigma$. (b) one single elastic NP of radius $R = 6\sigma$ with $k_{bend} = 0.001\epsilon$.

As noted by Shen et al.[5], the wrapping efficiency is determined by the receptors recruiting speed and the binding of ligands and receptors to overcome the energy barrier due to the membrane bending. In our case, the small sizes of the NPs and the high density of the receptors makes the recruiting speed of receptors not the dominant reason for different efficiency. Thus, only the difference in energy barrier for elastic NPs and rigid NPs are checked. The energy barrier of wrapping single soft NP contains the elastic energy change of the NP, the bending energy of the membrane and negligible changes of entropy due to the receptors. We check the relationships of

the energy with the wrapping ratio for NP with $R = 6\sigma$ with $k_{bend} = inf$ and $k_{bend} = 0.001\epsilon$ (Fig. S 9). As comparison, the bending energy of the lipid membrane wrapping rigid NP linearly increase as the wrapping ratio and finally reaches close to $8\pi\kappa$, which is next to the theoretical prediction. In contrast, the bending energy of the lipid membrane for wrapping elastic NP and the elastic energy of the soft NP increases first, then fluctuates and finally decreases slightly. The total energy barrier $\Delta E_{Barrier}$ for soft NP is larger than that of rigid NP at any wrapping ratio and is responsible for the slow endocytosis of elastic NPs.

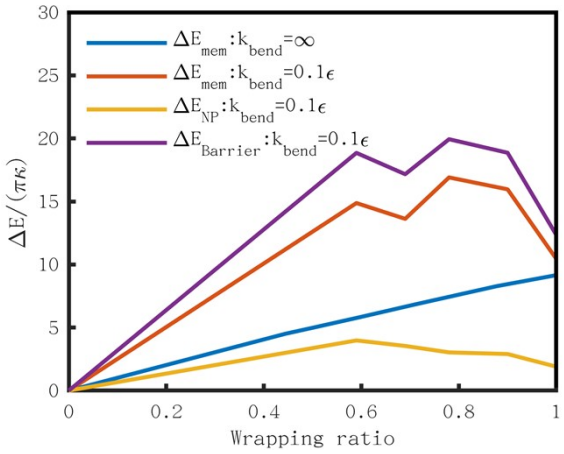

Fig. S 9 The relationship between the energy barrier and wrapping ratio for single NP with $R = 6\sigma$.

Next we analyze the wrapping efficiency of NPs from the perspective of the forces acting on the beads in the contact region between the NPs and lipid membrane. As shown in Fig. S 10, the contact lengths are almost indistinguishable from each other for the rigid and elastic NPs in the adhesion stage. However, the $\overline{f}_{centripetal}$ from the rigid NP is apparently bigger than that of the elastic NP before the NPs patching off from the membrane, reflecting a small energy barrier for rigid NP case. Even the $\overline{f}_z$ from the rigid NP don't show apparent superiority for $R = 6\sigma$ with $k_{bend} = 0.001\epsilon$. The persistent difference between the $\overline{f}_{centripetal}$ of the two situations promotes more ligand-receptor binding and results in higher wrapping efficiency for rigid NP. However, what is the reason for the difference in centripetal force between rigid NPs and soft NPs with similar contact length? As shown in Fig. S 11, the weaker

$\overline{f}_{centripetal}$ for elastic NP originates from the deformation of soft NPs, which makes the top end and bottom end of the soft NP sharpened and presents a gyroscopic shape. This relative configuration reduces the $\overline{f}_{centripetal}$ on the lipid membrane beads of the contact edges.

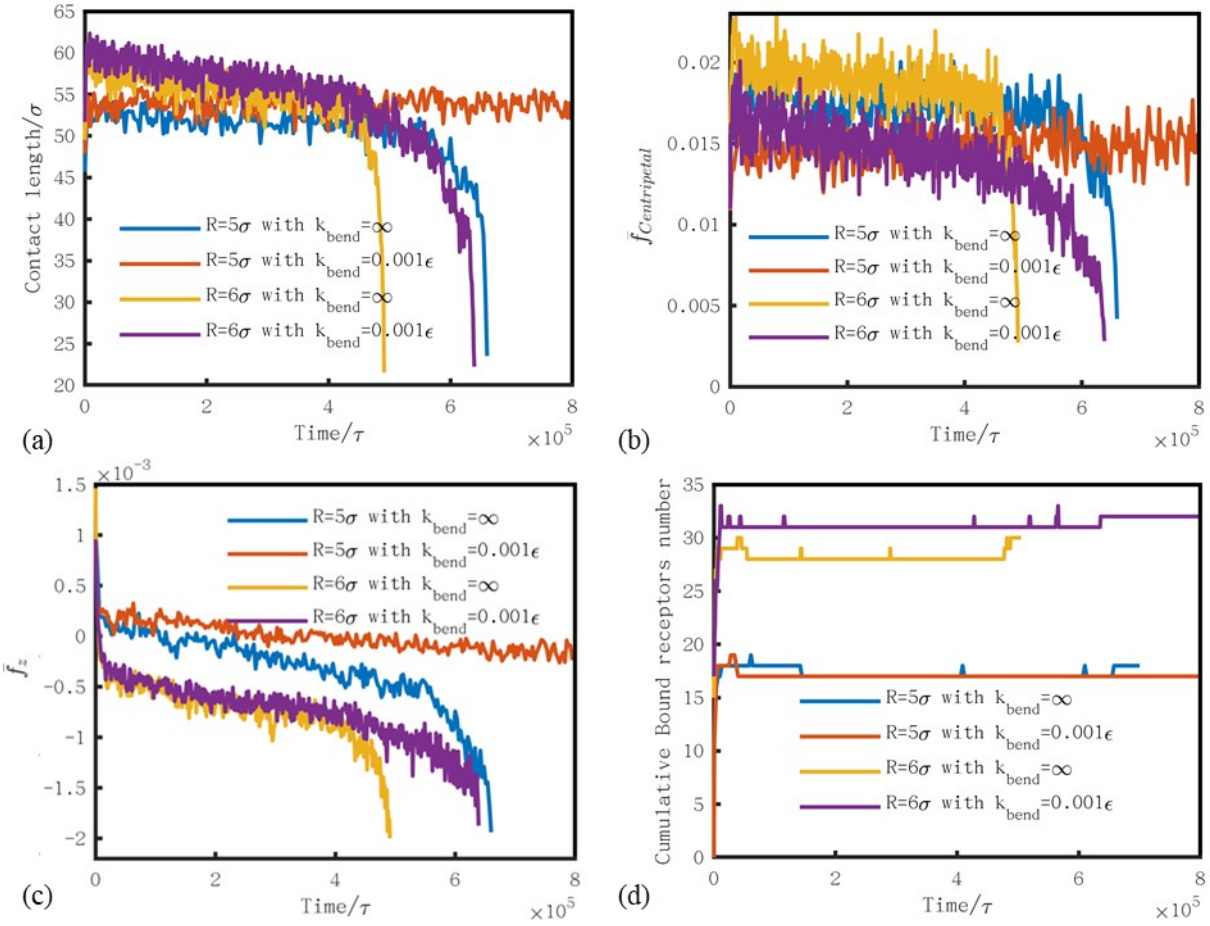

Fig. S 10 The interaction between single elastic NP with $R = 5\sigma$ or $R = 6\sigma$ and the phospholipid membrane. (a) Lengths of NPs and membrane contact edges. (b) $\overline{f}_{centripetal}$ on the beads on the contact edges. (c) $\overline{f}_z$ on the beads on the contact edges. (d) Cumulative number of receptor-ligand bonds.

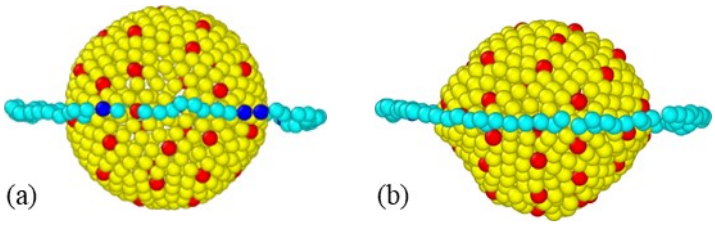

Fig. S 11 The position of the NP relative to the contact edge during wrapping. (a) Rigid NP with $R = 6\sigma$. (b) Elastic NP with $R = 6\sigma$ and $k_{bend} = 0.001\epsilon$.

The wrapping ratio evolution and the interactions of $R = 6\sigma$ with different k_{bend} are shown in Fig. S 12. With the bending rigidity of the NP decreasing, the eventually wrapping time increases monotonically due to the bigger energy barrier. The contact length, $\overline{f}_{centripetal}$, $\overline{f}_z$ and the cumulative bound receptor numbers are also shown in Fig. S 13. During the wrapping, the $\overline{f}_{centripetal}$ is bigger in the $\overline{f}_{centripetal}$ leading stage and $\overline{f}_z$ is bigger in the $\overline{f}_z$ leading stage for NPs with higher stiffness, which accelerate the wrapping.

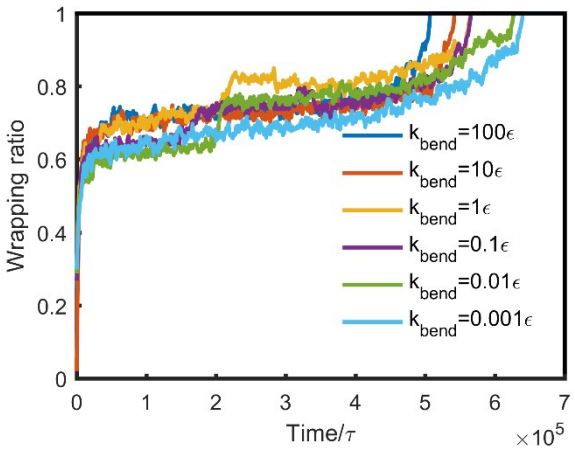

Fig. S 12 The wrapping ratio evolution and the interactions of $R = 6\sigma$ with different k_{bend}.

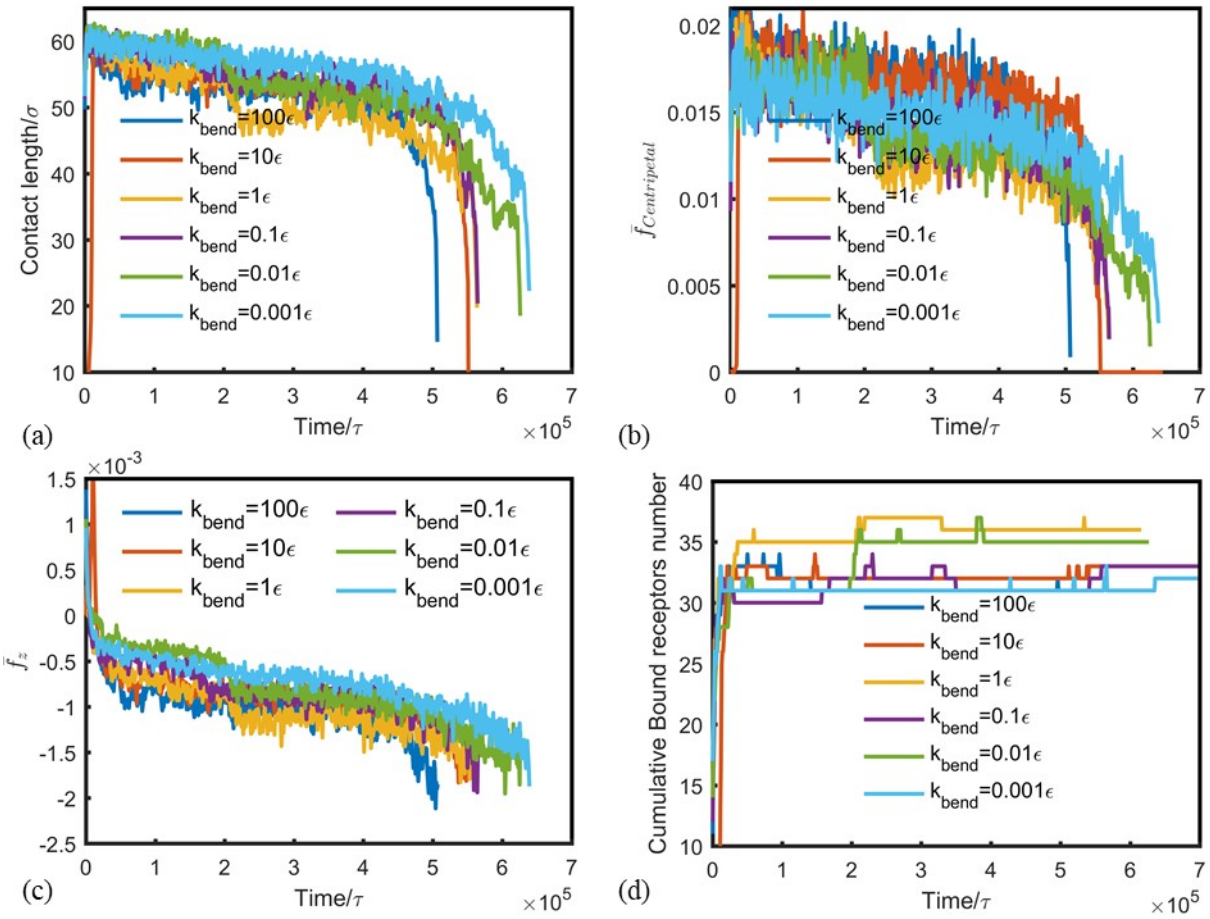

Fig. S 13 The interaction between single elastic NP with different k_{bend} and the phospholipid membrane. (a) Lengths of NP and membrane contact edges. (b) $\overline{f}_{centripetal}$ on the beads on the contact edges. (c) $\overline{f}_z$ on the beads on the contact edges. (d) Cumulative number of receptor-ligand bonds.

9. Cooperative wrapping of two elastic NPs.

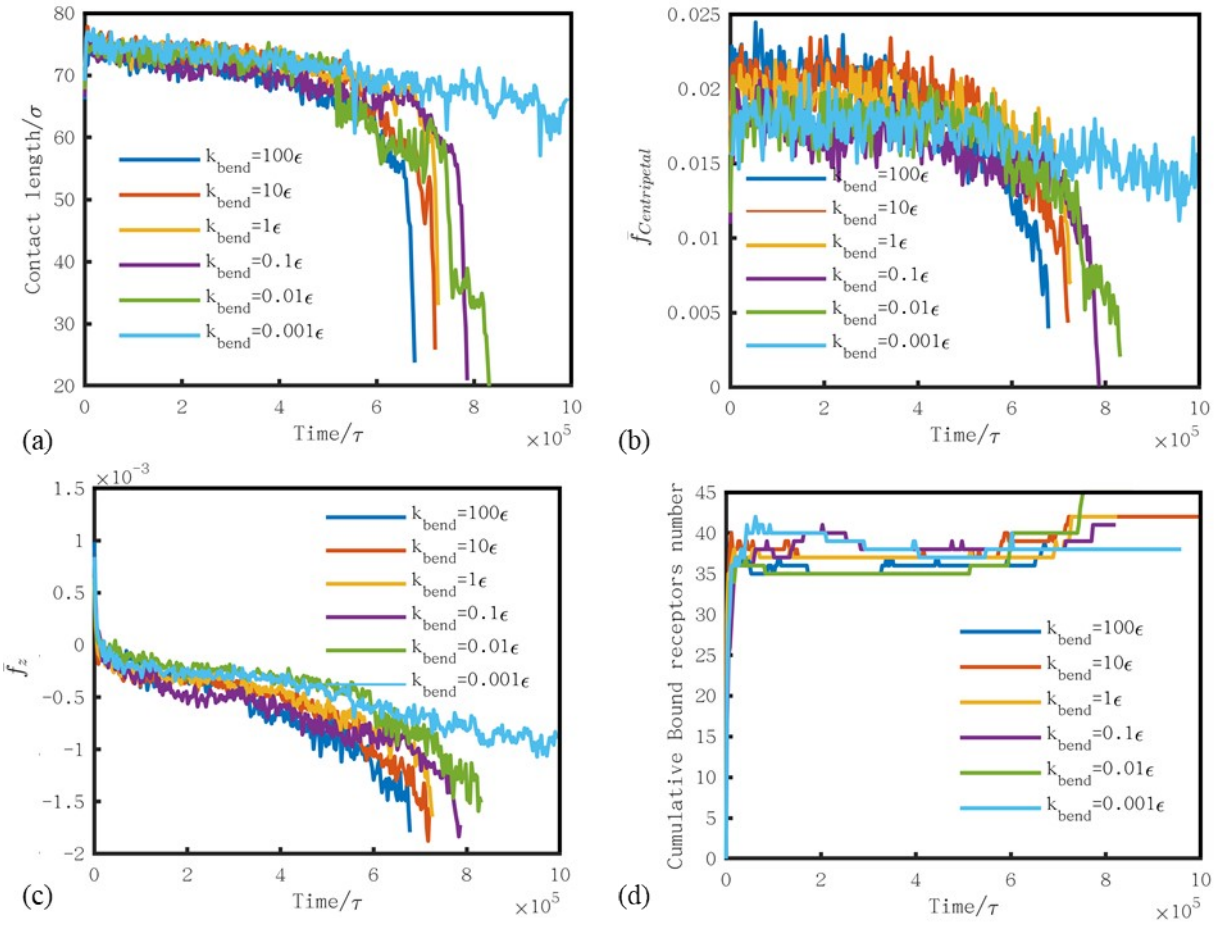

Fig. S 14 The interaction between two identical nanoparticles with different k_{bend} and the phospholipid membrane when $\epsilon_{NP-NP} = 0.02$. (a) Lengths of nanoparticles and membrane contact edges. (b) $\overline{f}_{centripetal}$ on the beads on the contact edges. (c) $\overline{f}_z$ on the beads on the contact edges. (d) Cumulative number of receptor-ligand bonds.

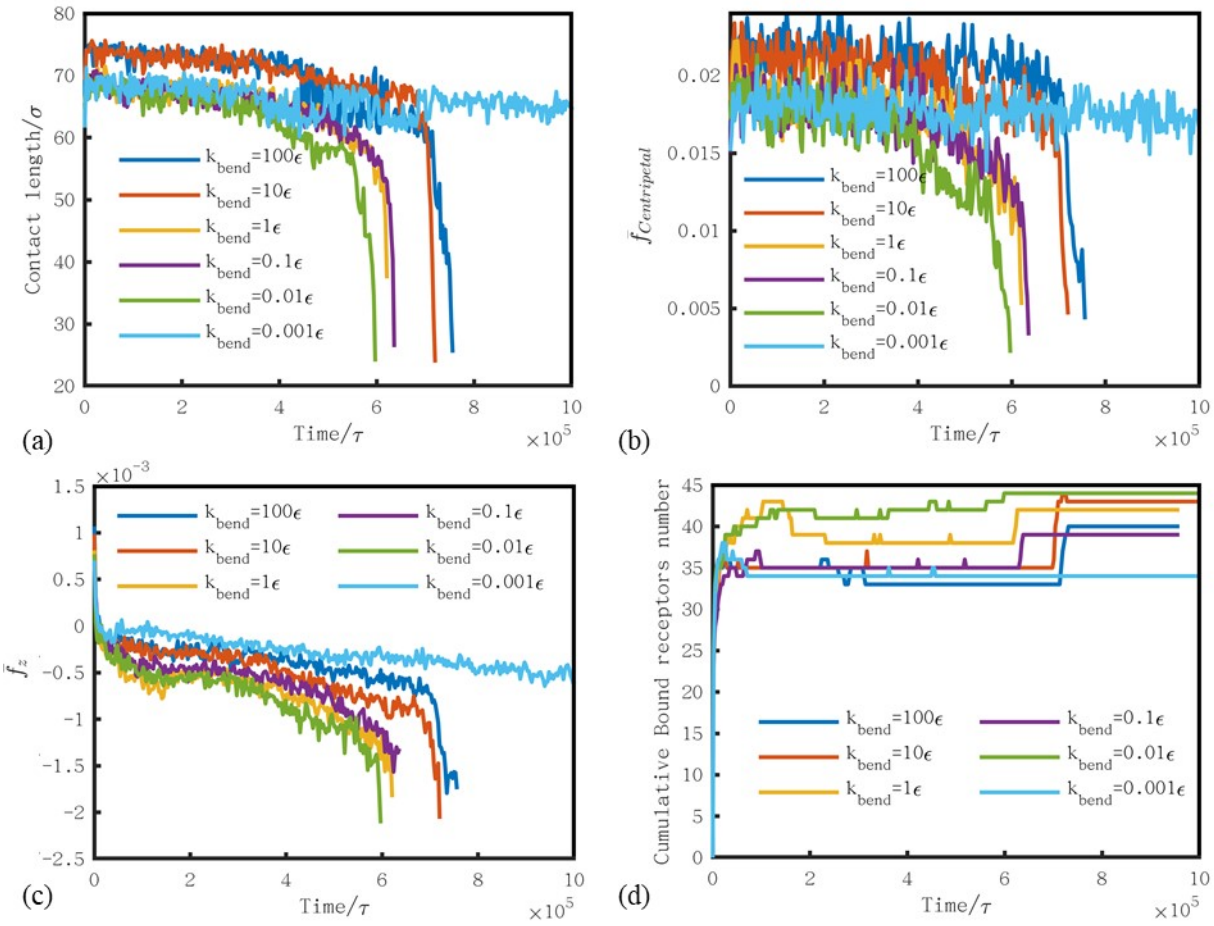

Fig. S 15 The interaction between two identical nanoparticles with different k_{bend} and the phospholipid membrane when $\epsilon_{NP-NP} = 0.2$. (a) Lengths of nanoparticles and membrane contact edges. (b) $\bar{f}_{centripetal}$ on the beads on the contact edges. (c) $\bar{f}_z$ on the beads on the contact edges. (d) Cumulative number of receptor-ligand bonds.

10. The bending energy of wrapping two NPs.

Unlike the single NP, the bending energy cannot be obtained by computing the energy using the geometry with curvatures same with the NP. Here we cut the lipid membrane by the contact edge with the NPs. By triangulation of the contact area with the lipid beads as the vertices, the bending energy of the re-created surface can be computed. Fig. S 16 shows the wrapping configuration of the two NPs with $k_{bend} = \infty$ and $k_{bend} = 0.1$ when $\epsilon_{NP-NP} = 0.02\epsilon$. The bending energy of the lipid membrane can be expressed using the Canham-Helfrich curvature energy functional[8]:

$$H_{el} = \frac{\kappa}{2}\int (2H - C_0)^2 dS \tag{12}$$

where κ is the bending rigidity of membrane and H is the mean curvature of the

surface. The spontaneous mean curvature $C_0 = 0$. The energy is the sum of the triangulation networks.

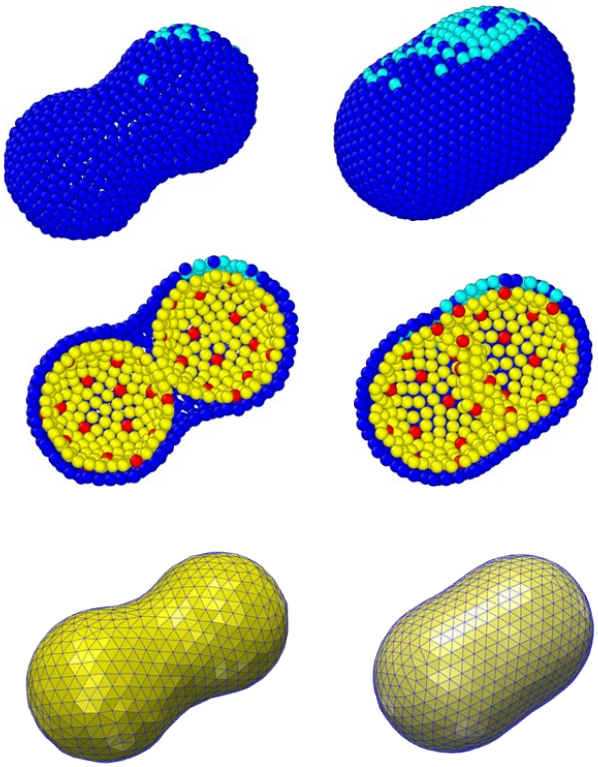

Fig. S 16 Transformation of cell membrane configuration from NPs to networks.

11. Cooperative wrapping of a combination of one rigid NP and one elastic NP

This section discusses the cooperative endocytosis efficiency of an ideal rigid NP and an elastic NP combination. The stiffness of the elastic NP changes from $k_{bend} = 0.001\epsilon$ to $k_{bend} = 100\epsilon$. Two cases with interaction strength of $\epsilon_{NP-NP} = 0.02$ and $\epsilon_{NP-NP} = 0.2$ between two NPs were considered.

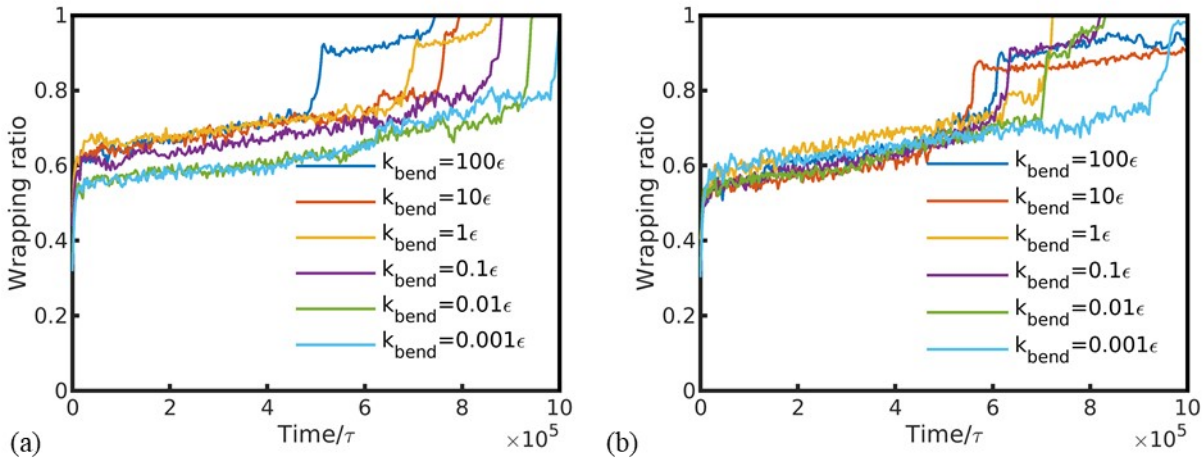

Fig. S 17 The wrapping ratio as function of time for a combination of one rigid NP and one elastic NP with different k_{bend}. (a) When $\epsilon_{NP-NP} = 0.2$. (b) When $\epsilon_{NP-NP} = 0.02$.

Fig. S 17 gives the cooperative wrapping ratio evolution for one rigid NP combined with a soft NP with different k_{bend} with $\epsilon_{NP-NP} = 0.02$ and $\epsilon_{NP-NP} = 0.2$. Basically, whether under strong or weak interactions, the combination of a rigid NP and a flexible NP increases the endocytosis efficiency as the stiffness of the flexible NP decreases. Except for weak interactions, the combination of rigid NP and flexible NP with $k_{bend} = 0.001\epsilon$ and $k_{bend} = 0.01\epsilon$ cannot be fully wrapped. Like the previous conclusion about two elastic NPs, under strong interaction, flexible NPs are prone to deformation and adhere to the surface of rigid NP to form a whole. Compared to the increase in energy barrier caused by the flexibility of the soft NP, which hinders endocytosis, the geometric configuration is more conducive to endocytosis, thereby improving the endocytosis efficiency. The contact length, $\overline{f}_{centripetal}$, $\overline{f}_z$ and the cumulative bound receptor numbers when $\epsilon_{NP-NP} = 0.2$ are shown in Fig. S 18. Under weak interactions, different from the wrapping of two elastic NPs, the interaction between the rigid NP and the elastic NP is enough to cause one single elastic NP deformation and combine the two NPs into a whole. For the whole combination, the lipid membrane can first wrap the rigid NP, which requires a lower energy barrier to overcome and at the same time, the weak interactions may alter the shape of the flexible NP, promoting a tighter binding between the two NPs. Therefore, even if the interaction is weak, the endocytosis efficiency of the combination of rigid NP and flexible NP will still increase as the stiffness of the nanoparticles decreases. The contact length, $\overline{f}_{centripetal}$, $\overline{f}_z$ and the cumulative bound receptor numbers when $\epsilon_{NP-NP} = 0.02$ are shown in Fig. S 19. NPs with fast internalization always generate greater $\overline{f}_z$.

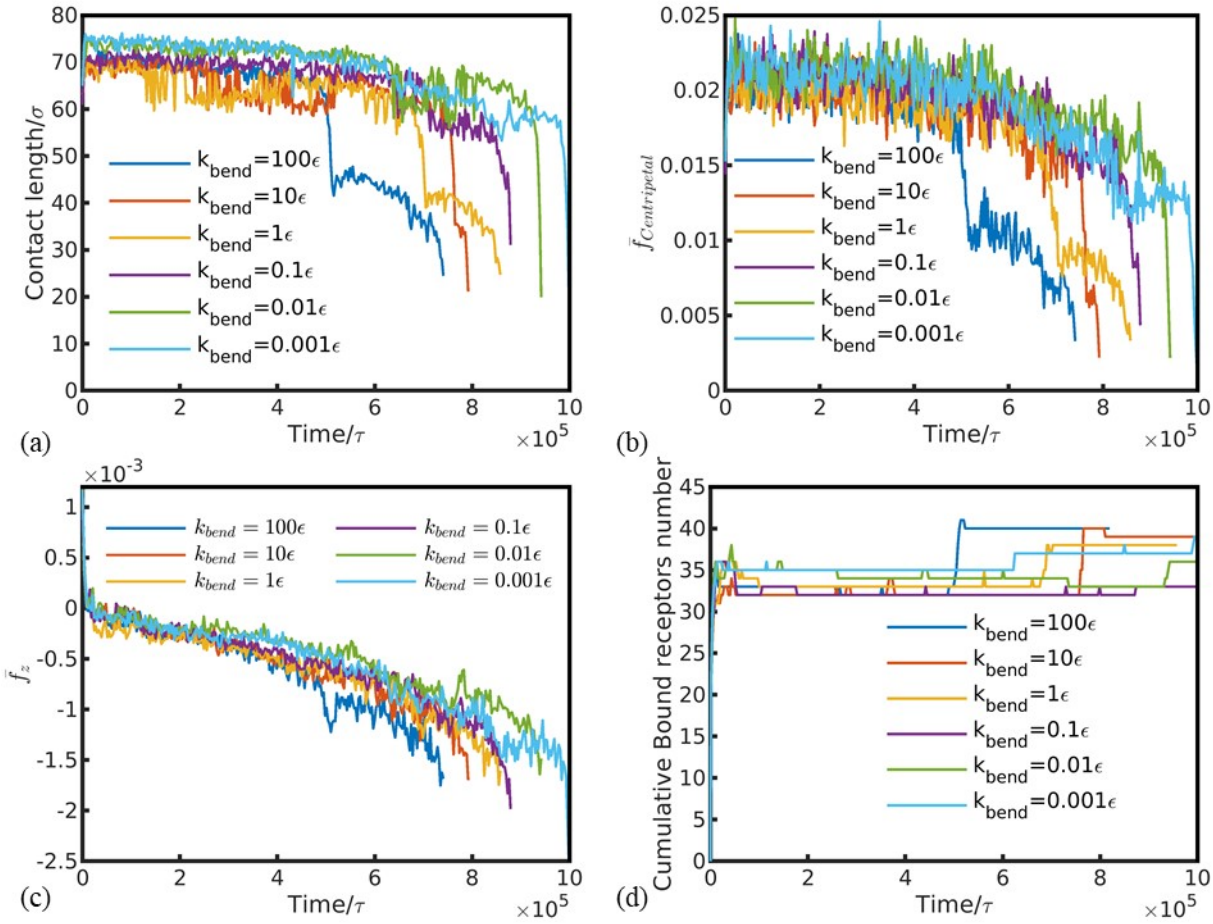

Fig. S 18 The interaction between a combination of one rigid NP and one elastic NP with different k_{bend} and the phospholipid membrane when $\epsilon_{NP-NP} = 0.2$. (a) Lengths of nanoparticles and membrane contact edges. (b) $\overline{f}_{centripetal}$ on the beads on the contact edges. (c) $\overline{f}_z$ on the beads on the contact edges. (d) Cumulative number of receptor-ligand bonds.

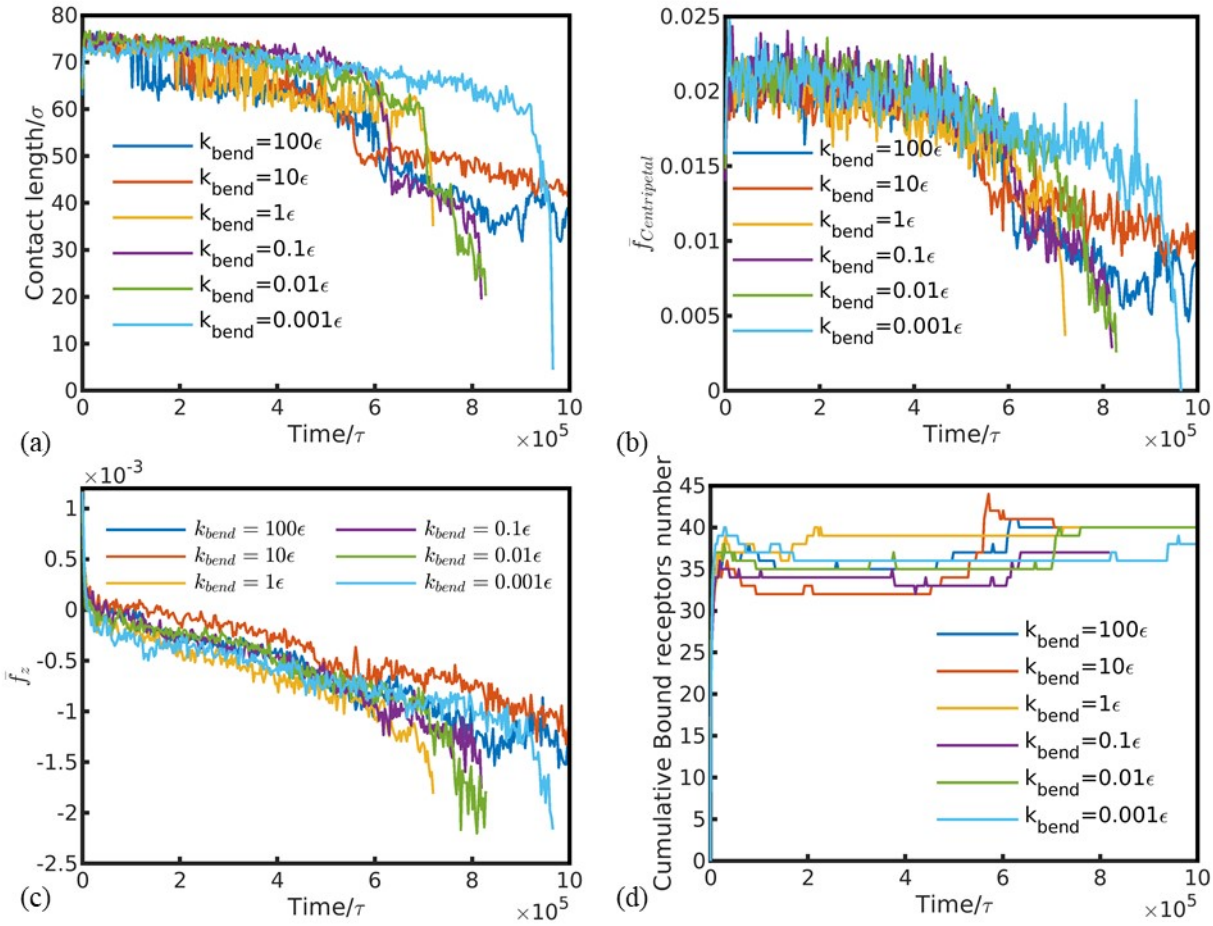

Fig. S 19 The interaction between a combination of one rigid NP and one elastic NP with different k_{bend} and the phospholipid membrane when $\epsilon_{NP-NP} = 0.02$. (a) Lengths of nanoparticles and membrane contact edges. (b) $\overline{f}_{centripetal}$ on the beads on the contact edges. (c) $\overline{f}_z$ on the beads on the contact edges. (d) Cumulative number of receptor-ligand bonds.

12. Two NPs with different ligands for targeting application

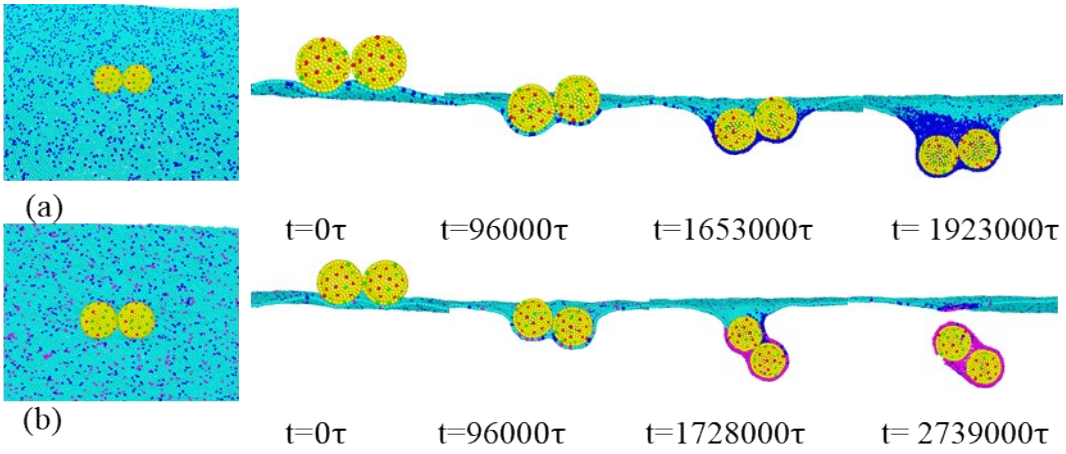

Fig. S 20 Combination of NP_c - NP_C interacting with two types membrane (a) *M1* and (b) *M2*. The $NP_C - NP_C$ adhere to the surface of *M1* and can be fully engulfed by *M2*.

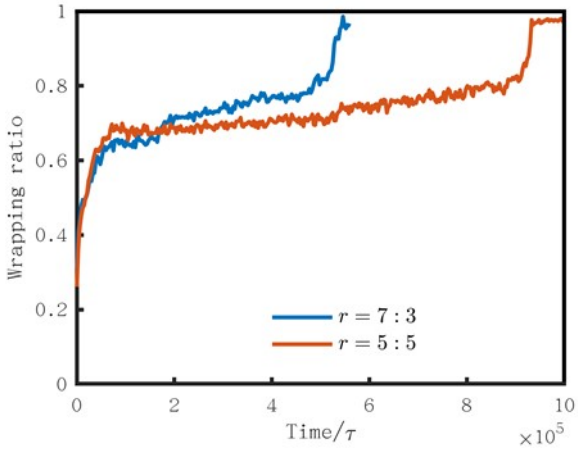

Fig. S 21 The wrapping ratio as function of time for combination of $NP_A - NP_B$ (a) When $r = 5{:}5$. (b) When $r = 7{:}3$.

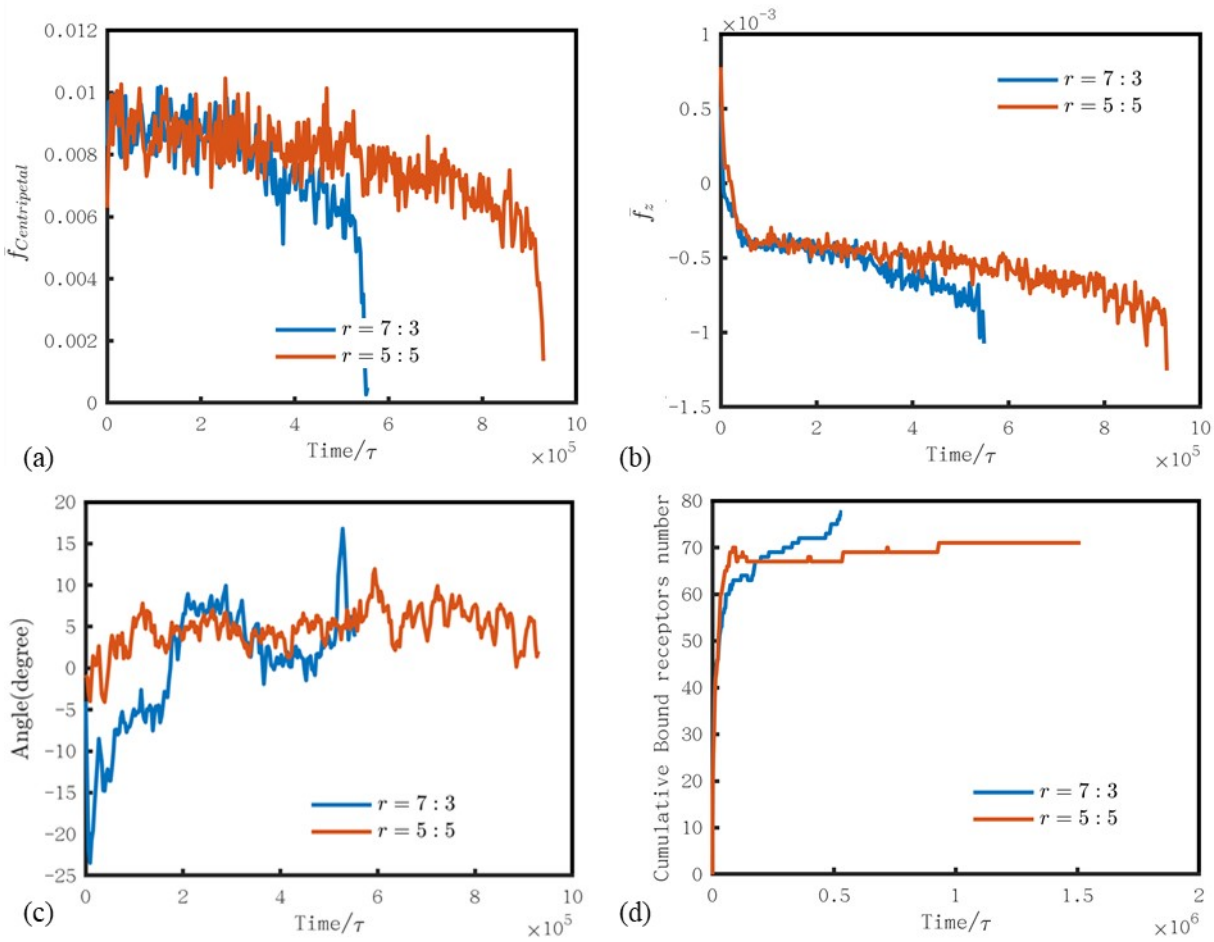

Fig. S 22 The interaction between the composite nanoparticles and the phospholipid membrane when $r = 5{:}5$ and $r = 7{:}3$. (a) $\overline{f}_{centripetal}$ on the beads on the contact edges. (b) $\overline{f}_z$ on the beads on the contact edges. (c) The angle between the line connecting the centers of the two NPs and the plane of the phospholipid membrane. (d) Cumulative number of receptor-ligand bonds.

Reference

1. Yuan, H.Y., C.J. Huang, and S.L. Zhang, *Dynamic shape transformations of fluid vesicles.* Soft Matter, 2010. **6**(18): p. 4571-4579.
2. Yuan, H., et al., *One-particle-thick, solvent-free, coarse-grained model for biological and biomimetic fluid membranes.* Phys Rev E Stat Nonlin Soft Matter Phys, 2010. **82**(1 Pt 1): p. 011905.
3. Chen, L., et al., *Morphological and mechanical determinants of cellular uptake of deformable nanoparticles.* Nanoscale, 2018. **10**(25): p. 11969-11979.
4. Li, J., et al., *Spectrin-Level Modeling of the Cytoskeleton and Optical Tweezers Stretching of the Erythrocyte.* Biophysical Journal, 2005. **88**(5): p. 3707-3719.
5. Shen, Z., et al., *Membrane Wrapping Efficiency of Elastic Nanoparticles during Endocytosis: Size and Shape Matter.* ACS Nano, 2019. **13**(1): p. 215-228.
6. Shen, Z., H. Ye, and Y. Li, *Understanding receptor-mediated endocytosis of elastic nanoparticles through coarse grained molecular dynamic simulation.* Phys Chem Chem Phys, 2018. **20**(24): p. 16372-16385.
7. Hui, Y., et al., *Nanoparticle elasticity regulates phagocytosis and cancer cell uptake.* Sci Adv, 2020. **6**(16): p. eaaz4316.
8. Helfrich, W., *Elastic properties of lipid bilayers: theory and possible experiments.* Z Naturforsch C, 1973. **28**(11): p. 693-703.